

# STUDY ON THE ALGORITHM OF INVERSING SEA SURFACE SALINITY BASED ON LANDSAT8/OLI DATA

Sun Zhen<sup>1</sup>, Huang Miaofen<sup>2\*</sup>, Wang Zhonglin<sup>3</sup>, Zhuang Yang<sup>4</sup>, Huang Ying'en<sup>5</sup>, Sun Zhongyong<sup>6</sup>, Zhang Tao<sup>7</sup>.

<sup>1</sup> Dalian Ocean University, No. 52, Heishijiao Street, Shahekou District, Dalian 116023, China,  
Email: sz\_0224@163.com

<sup>2\*</sup> Guangdong Ocean University, No. 1, Haida Street, Mazhang District, Zhanjiang 524088, China,  
Email: hmf808@163.com

<sup>3</sup> Dalian Ocean University, No. 52, Heishijiao Street, Shahekou District, Dalian, 116023 China,  
Email: wzllin@126.com

<sup>4</sup> Guangdong Ocean University, No. 1, Haida Street, Mazhang District, Zhanjiang, 524088 China,  
Email: 418514569@qq.com

<sup>5</sup> Guangdong Ocean University, No. 1, Haida Street, Mazhang District, Zhanjiang, 524088 China,  
Email: 492354130@qq.com

<sup>6</sup> Guangdong Ocean University, No. 1, Haida Street, Mazhang District, Zhanjiang, 524088 China,  
Email: sun\_idea@163.com

<sup>7</sup> Guangdong Ocean University, No. 1, Haida Street, Mazhang District, Zhanjiang, 524088 China,  
Email: 18840861947@163.com

**KEY WORDS:** Sea surface salinity, Colored dissolved organic matter, The Pearl River Estuary, Landsat 8/OLI, Remote sensing algorithm.

**ABSTRACT:** SSS (Sea Surface salinity) is an important parameter to describe the physical state of the ocean. It's necessary for gaining a better understanding of ocean circulation, global water cycle and climate change to study the distribution and variation features of the sea surface salinity. In nowadays, the various countries' scholars have made lots of study on the algorithm of inversing SSS by the method of microwave remote sensing. But due to its own complicated environment, inversing SSS in the estuarine coastal waters by the microwave remote sensing technique suffers some obstacles. CDOM (Colored dissolved organic matter) is the optical active ingredient of Dissolved Organic Matter in sea water, it is one of the three optical properties compositions which can be detected by ocean color remote sensing. A great deal of scientific research proved that CDOM in coastal waters is mainly affected by terrestrial input. To a certain extent, it can represent fresh water injection amount, so it is generally negatively correlated with salinity. It provides the feasibility for inversing the sea surface salinity by the visible-near infrared remote sensing. We obtained large amounts of the field experimental data. These data includes the sea surface salinity measured by CTD and the absorption coefficient of CDOM and water spectrum data at 28 stations in the region of the Pearl River Estuary in November 2013 and February 2014. After analyzing the quantitative relationship between SSS and the absorption coefficient of CDOM, an empirical algorithm for the inversion of SSS in the estuary waters with the absorption coefficient of CDOM based on Landsat8/OLI images data was established. The algorithm was applied in the region of the Pearl River Estuary. Obtain the spatial distribution thematic maps of the sea surface salinity in this area.

## 1. INTRODUCTION

Sea surface salinity is one of the key variables to describe the basic properties of the ocean. It not only has a critical role in the global water cycle and ocean circulation, but also one of the crucial factors determining the marine organisms living environment and marine primary productivity. With the features of observing large area continuously, synchronously and timely, using the remote sensing technique to observe sea surface salinity is the most effective way at present which could meets the great needs of using this parameter in various fields study. In nowadays, the various countries' experts and scholars have made lots of study on the algorithm of inversing the sea surface salinity by the method of microwave remote sensing (Burrage, 2008; Yueh, 2012). It has proved that the superiority of the microwave remote sensing used in quantitative analysis. But due to its own complicated environment, inversing the sea surface salinity in the estuarine coastal waters by the microwave remote sensing technique suffers some obstacles.

---

\*Corresponding author: [hmf808@163.com](mailto:hmf808@163.com)

Sea surface salinity is not the photosensitive material and the ability to absorb and diffuse the light in natural waters is weak. So it is difficult to extract the sea surface salinity from the remote sensing data. At present, some scholars build relationships between the sea surface salinity and the spectra information based on the statistical analysis of different band combinations (Wang, 2008; Man, 2007). Some other scholars make the study on the relationship between the photosensitive materials and sea surface salinity, Bowers proposed that there is a close relationship between the sea surface salinity and photosensitive materials (total suspended sediment and colored dissolved organic matter)(Bowers, 2000).

CDOM is the optical active ingredient of Dissolved Organic Matter in sea water and it is one of the three optical properties compositions which can be detected by ocean color remote sensing. A great deal of scientific research proved that CDOM in coastal region is mainly affected by terrestrial input. CDOM in ocean is mainly produced by self-degradation of marine organisms and the marine production of the bottom sediments release, the concentration of this part is low. So concentration of CDOM in the estuarine coastal waters can represent fresh water injection amount, so it is generally negatively correlated with salinity. It provides the feasibility for inverting the sea surface salinity by the visible-near infrared remote sensing.

After the two sea trials, we obtained the large amounts of data including the absorption coefficient of CDOM and the sea surface salinity measured by CTD and the water spectrum data in the Pearl River Estuary to establish a remote sensing algorithm based on Landsat8/OLI to extract the sea surface salinity, and its application in the Pearl River Estuary. Obtain the spatial distribution thematic maps of the sea surface salinity in this area and analyze the spatial and temporal variation of SSS in the Pearl River Estuary.

## 2. MATERIALS AND METHOD

### 2.1 Study Area

In this paper, study area is the Pearl River Estuary and the surrounding waters including the coastal region of eight estuary entrance and the region near the South China Sea(22° 45′ N, 113° E~21° 15′ N, 114° E). There were twenty eight sampling stations in the area. The experiment divided into two cruise. Sampling time was arranged in November 2013 (winter) and February 2014 (spring). Station distribution is shown in Figure 1.

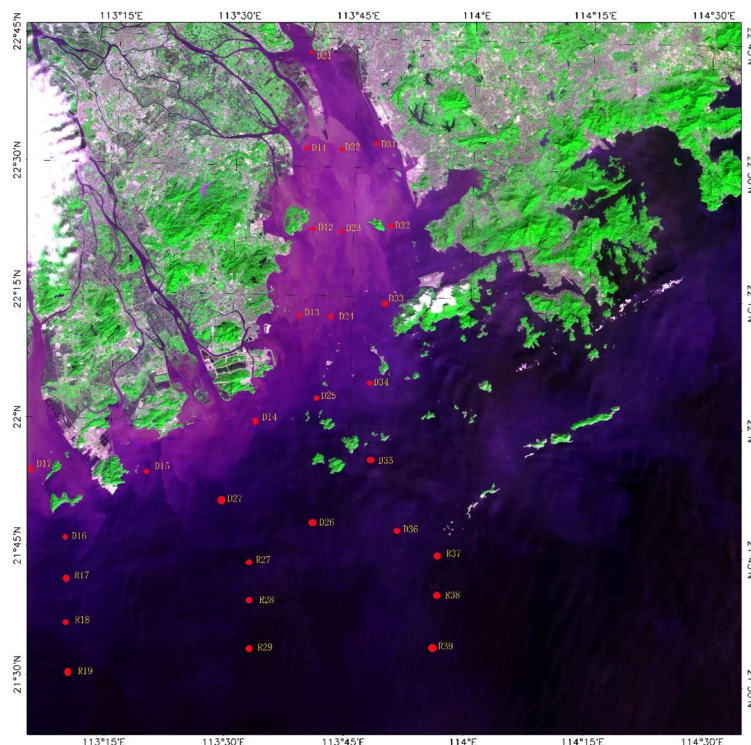


Figure 1. Sampling stations distribution in the Pearl River Estuary

Due to the adverse sea condition in the winter of 2013, the data of some sampling stations which are mainly near the South China Sea were not available. We obtained the experimental data in-situ including the absorption coefficient of CDOM, the sea surface salinity and water spectrum information. The number of effective samples of CDOM is 46. The number of effective samples of water spectrum data is 33.

## 2.2 Experimental Method

### 2.2.1 The Measurement of the Apparent Optical Parameters

The instrument used for measuring the apparent optical properties is ASD FieldSpec3 (350nm~2500nm). The method of measuring in Case II Waters is Above-Water Method. Select the reflectance of gray board is 0.3 as the reference board. The order of measuring is board, water, sky, board. The number of the spectra data is 15 spectral curve each group, the sampling interval of the two data is 1s (Huang, 2011).

Eq. (1) is used to compute the total radiance detected by radiometer:

$$L_{\text{sfc}}(\lambda, \theta; \theta_0, \varphi_0) = L_{\text{W}}(\lambda, \theta, \varphi; \theta_0, \varphi_0) + \rho \cdot L_{\text{sky}}(\lambda, \theta, \varphi; \theta_0, \varphi_0) + \Delta \quad (1)$$

Where,  $L_{\text{sfc}}$  is the total radiance detected by radiometer ( $\text{Wm}^{-2} \cdot \text{sr}^{-1} \cdot \mu\text{m}^{-1}$ );  $L_{\text{W}}$  is water leaving radiance ( $\text{Wm}^{-2} \cdot \text{sr}^{-1} \cdot \mu\text{m}^{-1}$ );  $L_{\text{sky}}$  is sky light radiance ( $\text{Wm}^{-2} \cdot \text{sr}^{-1} \cdot \mu\text{m}^{-1}$ );  $\rho$  is Fresnel reflectance;  $\Delta$  is outside interference;  $\theta$  is the incidence angle,  $\varphi$  is the azimuth angle.  $\theta=40^\circ$ ,  $\varphi=135^\circ$ .

### 2.2.2 The Measurement of the Absorption Coefficient of CDOM

It is still a difficult problem to obtain the concentration of CDOM directly at present. Many researchers have analyzed CDOM's optical behaviors, they regarded the absorption coefficient of CDOM as the concentration of CDOM. During the cruise, it's possible to meet some uncertain factors. Determine the parallel sample at each station for reducing error. Each sample was measured twice times. Select one group from the four groups as the experimental data to ensure the measurement accuracy of data. The process of the experiment is in accordance with NASA's marine optical survey specification (Han, 2006).

Eq. (2) is used to compute the absorption coefficient of CDOM:

$$a_g(\lambda) = 2.303 / l [ [OD_s(\lambda) - OD_{\text{bs}}(\lambda)] - OD_{\text{null}} ] \quad (2)$$

Where,  $l$  is the inner wall spacing of the cuvette;  $OD_s(\lambda)$  is the optical density of samples compared with pure water (dimensionless);  $OD_{\text{bs}}(\lambda)$  is the optical density of the treated water compared with pure water (dimensionless);  $OD_{\text{null}}$  is the residual absorption of visible or near infrared (dimensionless).

### 2.2.3 The Measurement of the Sea Surface Salinity

CTD (Conductivity-Temperature-Depth system) is an instrument designed to measure water temperature, salinity, pressure and other parameters at the different depth or layer of the water. The data of sea surface salinity obtained in the Pearl River Estuary is measured by CTD. The sampling interval of the two data is 0.25s.

## 2.3 The Remote Sensing Data Sources

In this paper, the remote sensing data are from Landsat8/OLI. Landsat8 satellite was launched successfully on February 11, 2013. The data can be downloaded for free. Table 1 is the parameters of the OLI sensor (Li, 2013). The remote sensing images are captured on November 29, 2013. Path: 122, Row: 44-45.

Table 1. The band parametric settings of the Landsat8/OLI

Sensor name	band	wavelength/ $\mu\text{m}$
OLI	B1	0.433~0.453
	B2	0.450~0.515
	B3	0.525~0.600
	B4	0.630~0.680
	B5	0.845~0.885
	B6	1.560~1.660
	B7	2.100~2.300
	B8	0.500~0.680
	B9	1.360~1.380

### 3. RESULTS AND DISCUSSION

#### 3.1 The Optical Properties of CDOM

The absorption coefficient and spectral slope can expressed the optical properties of CDOM. Optical definition of CDOM is defined as the amount of attenuation of the beam at a certain wavelength. According to the rule that the spectral absorption strength of CDOM decreased exponentially with the increase of wavelength in the range of 350-700nm wavelength, absorption spectrum curve of the exponential algorithm can be used for simulation (Bricaud, 1981).

Eq. (3) is used to compute the absorption coefficient of CDOM:

$$a_g(\lambda) = a_g(\lambda_0) \cdot e^{-S(\lambda-\lambda_0)} \quad (3)$$

Where,  $\lambda$  is the selected wavelength (nm),  $\lambda_0$  is the reference wavelength (nm),  $a_g(\lambda)$  is the absorption coefficient of CDOM at the selected wavelength of  $\lambda$ ,  $a_g(\lambda_0)$  is the absorption coefficient of CDOM at the selected wavelength of  $\lambda_0$ ,  $S$  is index spectral slope.

In this paper, the remote sensing algorithm of  $a_g(440)$  is the main research. The value of  $\lambda_0$  is different in different research fields. According to Eq. (3), the spectral absorption strength of CDOM decreased exponentially with the increase of wavelength, so absorption spectrum of CDOM will exhibit a high value at the band of ultraviolet and blue. Take the noise-signal ratio and UV attenuation caused by CDOM in the natural water bodies into consideration, the wavelength of  $\lambda_0$  is usually 250nm. In freshwater area, the wavelength of  $\lambda_0$  is usually 380nm, 375nm and 280nm. In coastal waters, there is a large error on the atmospheric correction at the band of short wavelength. There is an absorption overlap between CDOM and phytoplankton pigments at the band of blue, so  $\lambda_0$  is usually 440nm (Zhu, J. H., 2002).

Index spectral slope is mainly affected by CDOM composition and band selection, there is no concentration between  $S$  and the concentration of CDOM. There are a few researches proved the index spectral slope was greatly influenced by the regional conditions (Ma, 2005; Chen, 2012; Zhou, 2005).

Bringing the data which were obtained in November 2013 and February 2014 in the Pearl River Estuary waters into Eq. (3), and the reference wavelength is 440nm, and get the index spectral slope. The value of the index spectral slope is in the range of 0.009361-0.013859nm<sup>-1</sup>, the average of index spectral slope is 0.011878 nm<sup>-1</sup>.

#### 3.2 The Analysis of the Correlation between SSS and CDOM

Calculate the correlation coefficient between the sea surface salinity and other parameters including the index spectral slope,  $a_g(440)*S$ ,  $a_g(440)$ ,  $\ln[a_g(440)]$  and  $\ln[S*a_g(440)]$ . The highest correlation is between SSS and  $a_g(440)*S$ , followed by  $a_g(440)$ .

Table .2 is the correlation coefficient between SSS and other parameters.

Table 2. The correlation coefficient between SSS and other parameters

Index spectral slope	$a_g(440)$	$S$	$a_g(440)*S$	$\ln[a_g(440)]$	$\ln[S*a_g(440)]$
0.894	0.940	0.899	0.957	0.901	0.909

#### 3.3 Model Building of the Inversion of SSS

At present, as for the inversion of the concentration of CDOM, there are two kinds of the extraction of remote sensing model, the one is spectral indices method, based on remote sensing reflectance(Bowers, 2004), the other is the use of chlorophyll concentration and its absorption coefficient (Tehrani, 2013), based on the inherent optical properties (Gao, 2000). Bowers proposed it is feasible to use the reflectance ratio at the wavelength of 490nm and 670nm to estimate the absorption coefficient of CDOM in estuary region.

$$a_g(440)=1.45*(R(670)/R(490))-0.488 \quad (4)$$

This test is established on the basis of Bowers model proposed, using the measured water spectral data combined with Landsat8 / OLI response function, establishing CDOM remote sensing inversion model. Figure 2 is the fitting result of the model of the inversion of the absorption coefficient of CDOM at the wavelength of 440nm.

$$a_g(440)=0.0732*\exp(1.1827*(R4/R2)) \quad (R^2=0.83) \quad (5)$$

Where,  $R4$  and  $R2$  corresponds to the reflectance of the band4 (640 nm to 670 nm) and band2 (450 nm to 510 nm) of

Landsat8/OLI, respectively.

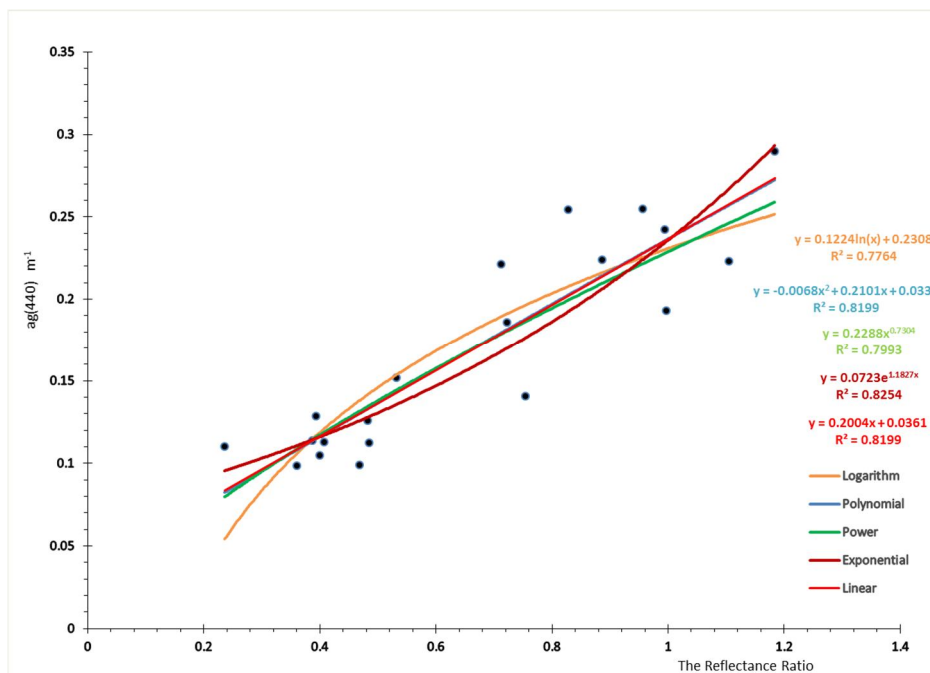


Figure 2. Fitting result of the inversion model of CDOM

Figure 3 is the fitting result of the model of the inversion of SSS. According to the quantitative relationship between CDOM and SSS, SSS remote sensing inversion model:

$$Y = -3 \times 10^6 X^2 + 4282.2X + 36.815 \quad (R^2 = 0.98) \quad (6)$$

Where, Y is the sea surface salinity; X is intermediate variable,  $X = S \cdot a_g(440)$ ; S is the index spectral slope;  $a_g(440)$  is the absorption coefficient of CDOM at the wavelength of 440nm.

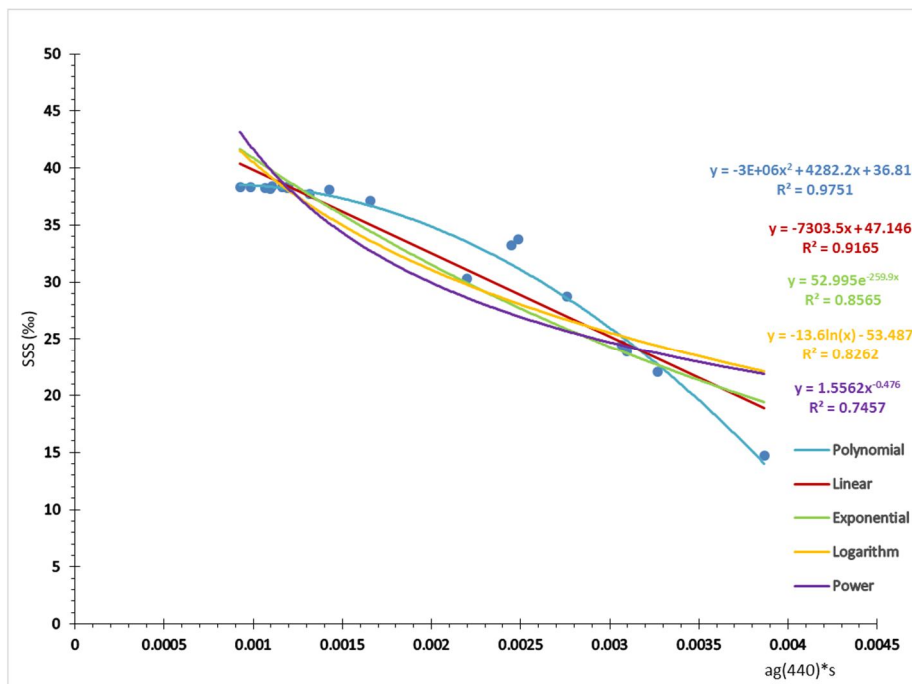


Figure 3. Fitting result of the inversion model of SSS

### 3.4 Application of the Model

#### 3.4.1 Remote Sensing Data Preprocessing

First of all, the remote sensing data should be processed by radiometric calibration. Due to the remote sensing image data based on grey value, grey value can't directly reflect the radiation characteristics of sea surface, so the first thing to do is to calibrate the radiation and convert the grey value of the original pixels into the apparent optical brightness. Then we must accurately remove the effects of atmospheric on it. In this test, use the FLAASH module in the software ENVI to correct the effect of atmospheric. At last, extract waters by the method of using the technique of NDWI (Normalized Difference Water Index) and setting the threshold.

#### 3.4.2 The Spatial Distribution Thematic Map of SSS

Figure 4 is the spatial distribution thematic map of the sea surface salinity in the Pearl River Estuary. The remote sensing data is obtained by Landsat8/OLI on November 29, 2011. According to the thematic map, there are a large number of rivers flow the fresh water into estuary in the northwest of the estuary. It makes that the salinity of western area is higher than the eastern area. The salinity of the water in coastal area is lower than the salinity of the water in ocean. The distribution of sea surface salinity is basically consistent with the actual situation of the estuary area. The experimental data obtained from two cruise also confirmed this point.

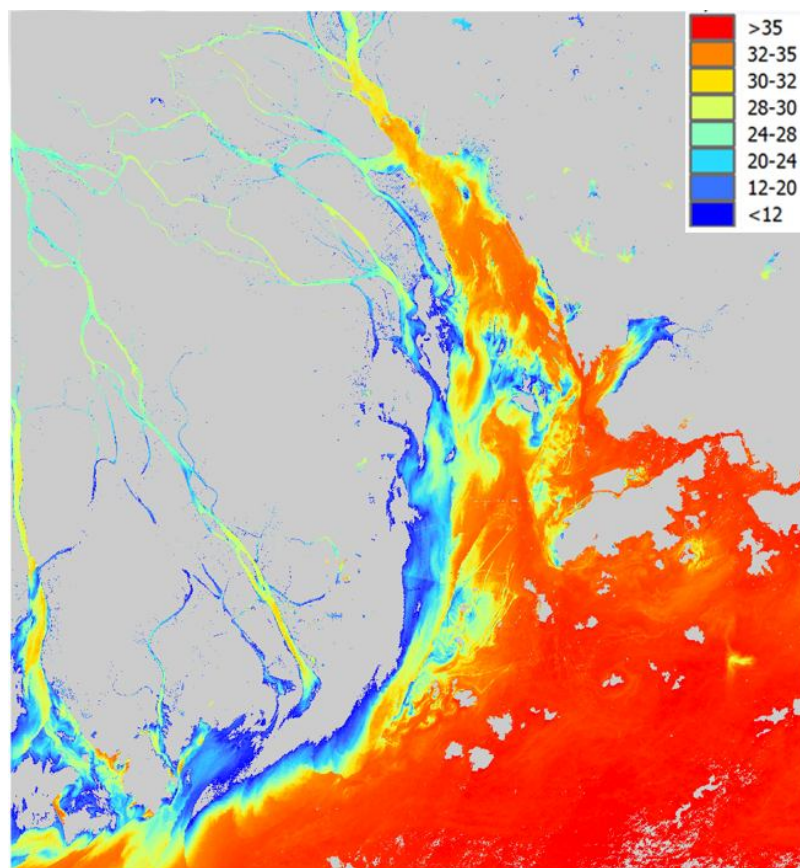


Figure 4. The spatial distribution thematic map of SSS

### 3.5 The Verification of the Model

Due to the actual situation, the satellite-ground synchronous experiment can't be achieved. The number of effective samples of water spectrum data is 33. 23 samples are used to simulate the remote sensing model of sea surface salinity. The others are used to verify the model. Figure 5 is the comparison chart of simulation value and actual value.



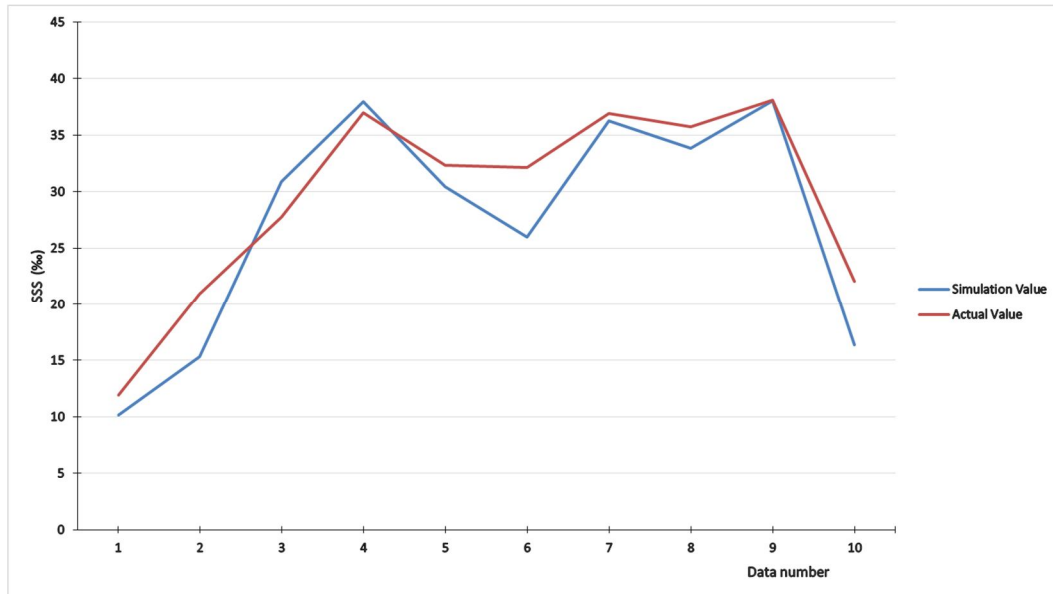


Figure 5. The Comparison Chart of Simulation Value and Actual Value

The algorithm of the inversion of SSS was applied into the Landsat8/OLI image captured on November 29, 2013. The distribution of sea surface salinity is basically consistent with the actual situation of the estuary area. Compare the calculated value from the inversion algorithm with the in-situ experimental data, the result shows simulation value are consistent with the in-situ experimental data, proved that the establishment of remote sensing mode has a certain credibility.

#### 4. CONCLUSION

According to the large amounts of data during the two cruises in the Pearl River Estuary, we established a remote sensing algorithm based on Landsat8/OLI to estimate SSS successfully. It is a new attempt and research to use optical remote sensing to estimate the sea surface salinity. The algorithm is an empirical algorithm. And CDOM is as an intermediary in the model, it makes the accuracy of the inversion of CDOM can affect the accuracy of the salinity inversion. The distribution of sea surface salinity is basically consistent with the actual situation of the estuary area. And compare the simulation value with the actual value, the result shows simulation value are consistent with the actual value, it proved that the establishment of remote sensing mode has a certain credibility. The verification of the model gets a good precision. These conclusions show it's feasible to select  $a_g(440)$  as the inversion factor to estimate the sea surface salinity in the estuarine waters.

#### ACKNOWLEDGEMENT

This work was funded by National Natural Science Foundation of China under contract No. 41271364, and supported by program for scientific research start-up funds of Guangdong Ocean University under contract No. E16187.

#### REFERENCES

- Bowers, D. G., 2000. Optical properties of a region of fresh water influence (the Clyde Sea). *Estuarine, Coastal and Shelf Science*, 50(5), pp. 717-726
- Bowers, D. G., Evans, D., Thomas, D. N., etc., 2004. Interpreting the colour of an estuary. *Estuarine Coastal and Shelf Science*, 59(1), pp.13-20.
- Bricaud, A., 1981. Absorption by dissolved organic matter of the sea (yellow substance) in the UV and visible domains. *Limnology & Oceanography*, 26(1), pp.43-53.
- Burrage, D., Wesson, J., Miller, J., 2008. Deriving Sea Surface Salinity and Density Variations from Satellite and Aircraft Microwave Radiometer Measurements: Application to Coastal Plumes Using STARRS. *Geoscience & Remote Sensing IEEE Transactions on*, 46(3), pp.765-785.
- Chen, X., Zhang, X. N., Lei, H., 2012. Optical absorption properties of CDOM and tracing implication of DOC in the Changjiang Estuary. *Marine Environmental Science*, 31(5), pp.625-630.
- Gao, B. C., Montes, M. J., Ahmad, Z., etc., 2000. Atmospheric correction algorithm for hyper spectral remote sensing

of ocean color from space. *Applied Optics*, 39(6), pp.887-896.

Han, J. X., Li, T. J., 2006. Marine optical investigation technical specification. Ocean Press, Beijing, pp.17-19.

Huang, M. F., Song, Q. J., Mao Z. H., 2011. The retrieval model for COD in waters using optical absorption properties of CDOM. *Acta Oceanologica Sinica*, 33(3), pp.47-54.

Li, X. W., Niu, Z. C., Jiang S., etc., 2013. Study on the usage of Landsat8 satellite remote sensing image in environment monitoring. *Environmental Monitoring and Forewarning*, 5(6), pp.1-5.

Ma, R. H., Dai, J. F., Zhang, Y. L., 2005. Influence factors and slope coefficients of absorption of colored dissolved organic matter (CDOM) in East Taihu Lake, China. *Journal of Lake science*, 17(2), pp.120-126.

Man, S. M., Kwon, H. L., 2008. Modeling of Suspended Solids and Sea Surface Salinity in Hong Kong using Aqua / MODIS Satellite Images. *Korean Journal of Remote Sensing*, 23(3), pp.161-169.

Tehrani, N. C., D'Sa, E. J., Osburn, C. L., 2013. Chromophoric Dissolved Organic Matter and Dissolved Organic Carbon from Sea-Viewing Wide Field-of-View Sensor (SeaWiFS), Moderate Resolution Imaging Spectroradiometer (MODIS) and MERIS Sensors: Case Study for the Northern Gulf of Mexico. *Remote Sensing*, 5(3), pp.1439-1464.

Wang, F. G., Xu., Y. J., 2008. Development and application of a remote sensing - based salinity prediction model for a large estuarine lake in the US Gulf of Mexico coast. *Journal of Hydrology*, 360(1-4), pp.184-194

Yueh, S. H., Chaubell, J., 2012. Sea Surface Salinity and Wind Retrieval Using Combined Passive and Active L-Band Microwave Observations. *IEEE Transactions on Geoscience & Remote Sensing*, 50(4), pp.1022-1032

Zhou, H. L., Zhu, J. H., Li, T. J., 2005. The analysis of water color element absorb spectral characteristic in Qinghai Lake. *Journal of Ocean Technology*, 24(2), pp.55-58.

Zhu, J. H., 2002. The selection of the reference wavelength of spectra absorption curve of yellow substance. *Ocean Technology*, 22(3), pp.10-14